Available online at www.sciencedirect.com
SCIENCE DIRECT®
Journal of Power Sources 124 (2003) 231–236
JOURNAL OF POWER SOURCES
www.elsevier.com/locate/jpowsour

Short communication

$LiTi_2(PO_4)_3$ with NASICON-type structure as lithium-storage materials

G.X. Wang*, D.H. Bradhurst, S.X. Dou, H.K. Liu

Battery Technology Research Program, Institute for Superconducting & Electronic Materials, University of Wollongong, Wollongong, NSW 2522, Australia

Received 19 March 2003; accepted 9 May 2003

Abstract

$LiTi_2(PO_4)_3$ with a Na^+ superionic conductor (NASICON)-type structure is prepared by a two-step solid-state reaction. X-ray diffraction (XRD) confirms that the $LiTi_2(PO_4)_3$ compound has a NASICON structure, i.e. rhombohedral (space group: *R*3*c*). It is found that lithium can be electrochemically inserted into the $LiTi_2(PO_4)_3$ structure, with a maximum intake of 5.2 mol of lithium per mole of $LiTi_2(PO_4)_3$ compound, and that $[PO_4]$ tetrahedra can participate in the redox reaction. This corresponds to a lithium-storage capacity of 360 mAh g^{-1}. The kinetic parameters of lithium insertion in $LiTi_2(PO_4)_3$ NASICON are determined by means of ac impedance technique. The charge-transfer resistance (R_{CT}) and exchange current density (i_0) are invariable regardless of the state of lithium insertion. This is associated with the unique structure characteristics of the NASICON skeleton. By contrast, the diffusion coefficient, D_{Li} of lithium varies with the state of lithium insertion. The value of D_{Li} is in the range 1.4×10^{-11} to 1.2×10^{-9} m^2 s^{-1}, which is much higher than for other intercalation materials.

Keywords: $LiTi_2(PO_4)_3$ NASICON; Lithium insertion; Impedance spectroscopy; Lithium-ion battery; Storage capacity; Diffusion coefficient

1. Introduction

The Na^+ superionic conductor (NASICON) materials are good ionic conductors when serving as solid-state electrolytes. The crystal structure of NASICON $A_xM_2(XO_4)_3$ consists of a network in which MO_6 octahedra share all their corners with XO_4 tetrahedra, and XO_4 tetrahedra, share all three corners with MO_6 octahedra. The interstitials and conduction channels are generated along the *c*-axis direction, in which alkali metal ions (Na^+ or Li^+) occupy the interstitial sites. Consequently, the alkali metal ions can move easily along the conduction channels [1–8].

The NASICON structure $A_xM_2(XO_4)_3$ can be chemically versatile. It can be stabilized with K^+, Na^+ or Li^+ in the A position, transition-metal cations in the M position, and P, Si or Mo in the XO_4 polyanions. Therefore, NASICON materials can be used not only as solid-state electrolytes, but also as lithium-storage materials in rechargeable lithium batteries, based on their structural characteristics [9–11]. The operation of Li-ion batteries relies on the diffusion of Li^+ ions in the cathode and anode hosts. Therefore, if a material host has good ionic conductivity, it will be very suitable as an electrode material for Li-ion batteries. The rate capacity of such batteries depends strongly on the diffusion of Li^+ ions. In this investigation, $LiTi_2(PO_4)_3$ has been synthesized and its electrochemical properties were investigated. The compound is a candidate anode material for Li-ion batteries because of the low potential of the Ti^{4+}/Ti^{3+} redox couple versus Li/Li^+.

2. Experimental

2.1. Synthesis and characterization of $LiTi_2(PO_4)_3$

The raw materials Li_2CO_3 (ACS reagent, Aldrich), TiO_2 (99.9%) and $(NH_4)\cdot H_2PO_4$ (ACS reagent, Aldrich) were thoroughly mixed with pestle and mortar. The resulting mixtures were then pressed into pellets and pre-calcined at 900 °C for 12 h to decompose Li_2CO_3 and $(NH_4)H_2PO_4$. The pellets were then reground and fired at 1250 °C for 24 h. The overall reaction is as follows:

$$0.5Li_2CO_3 + 2TiO_2 + 3(NH_4)H_2PO_4 \rightarrow LiTi_2(PO_4)_3 + 3NH_3 + 4.5H_2O + 0.5CO_2 \quad (1)$$

The synthesized $LiTi_2(PO_4)_3$ powders were characterized by X-ray diffraction (XRD) using a Philips PW 1010 X-ray diffractometer with Cu Kα radiation.

* Corresponding author. Fax: +61-2-42215731.
E-mail address: gwang@uow.edu.au (G.X. Wang).

0378-7753/$ – see front matter © 2003 Elsevier B.V. All rights reserved.
doi:10.1016/S0378-7753(03)00609-8

2.2. Electrochemical tests

Li|$LiPF_6$ (ethylene carbonate (EC) + dimethyl carbonate (DMC))|$LiTi_2(PO_4)_3$ coin cells (CR2032) were assembled to examine the lithium insertion properties of $LiTi_2(PO_4)_3$. The electrodes were made by dispersing a mixture of 85 wt.% active materials, 12 wt.% carbon black and 3 wt.% polyvinylidene fluoride (PVDF) binder in dimethyl phthalate (DMP) solvent to form a slurry. The slurry was then spread on to copper foil ($\phi = 12$ mm). The electrodes were dried at 1400 °C under vacuum for 24 h. The electrolyte was 1 M $LiPF_6$ in a mixture of EC and DMC (Battery Grade, Merck KGaA, Germany). The cells were assembled using a hand-operated closing tool (Hosen Corp., Japan) in an argon-filled glove-box (Unilab, Mbraun, USA) in which the oxygen and moisture were controlled to less than 1 ppm. The lithium test cells were discharged and charged at a constant current density of 0.1 mA cm^{-2} in a voltage window of either 0–2.5 or 0.25–1.2 V.

To determine the kinetic process of lithium insertion in the $LiTi_2(PO_4)_3$ compound, ac impedance measurements were performed on a $LiTi_2(PO_4)_3$ electrode in different states of discharge (SoD). The measurements were performed with an EG&G Princeton Applied Research Electrochemical Impedance Analyser (Model 6310). The test cell for ac impedance measurements consisted of three electrodes with lithium as counter electrode and reference electrode. The ac amplitude was 5 mV and the frequency range was 65 kHz to 1 mHz.

3. Results and discussion

$LiTi_2(PO_4)_3$ has a rhombohedral (space group: *R*3*c*) structure with an open three-dimensional framework of TiO_6 octahedra sharing all corners with PO_4 tetrahedra and vice versa. Li^+ ions occupy the interstitial spaces, either 18e or 6b sites. The XRD pattern of $LiTi_2(PO_4)_3$ is shown in Fig. 1. All diffraction lines are indexed based on a rhombohedral structure with a space group of *R*3*c*. The lattice constants are calculated to be $a = 8.5105$ Å and $c = 20.8645$ Å using a least-squares method for 25 diffraction lines. The calculated parameters of the unit cell are in good agreement with the literature value [12]. No XRD peaks correspond to the reagents or other impurity phases.

Li|$LiTi_2(PO_4)_3$ cells were discharged and charged at a constant current density of 0.1 mA cm^{-2} (20 mA g^{-1}). Lithium insertion into the $LiTi_2(PO_4)_3$ electrode corresponds to the discharge process, and the extraction of lithium from the host as the charge process. Discharge–charge profiles of one of the Li|$LiTi_2(PO_4)_3$ cells in the voltage range 0–2.5 V are shown in Fig. 2. The first lithiation for the $LiTi_2(PO_4)_3$ compound reached a capacity of 360 mAh g^{-1} which corresponds to an insertion of 5.2 mol of lithium per mole of $LiTi_2(PO_4)_3$. Only 65% of the initially inserted lithium could, however, be reversibly extracted in the first charge process. The capacity of $LiTi_2(PO_4)_3$ faded quickly with cycling. The charge and discharge capacity of the $LiTi_2(PO_4)_3$ electrode was mainly within the voltage range 0.1–0.8 V. This is different from $Li_4Ti_5O_{12}$ which has a potential of around 1.5 V versus Li/Li^+ [13,14]. If it is only the Ti^{4+}/Ti^{3+} redox couple which contributes to the redox reaction as lithium is inserted and extracted, then the operating potential should be almost the same for these two compounds. The experimental observation is opposite. Furthermore, if only the Ti^{4+} ions in $LiTi_2(PO_4)_3$ accept electrons associated with lithium insertion, the maximum lithium intake would be merely 2 mol of Li per mole of $LiTi_2(PO_4)_3$ to form $Li_3Ti_2(PO_4)_3$, whereas, approximate 5.2 mol of Li were electrochemically inserted per mole of $LiTi_2(PO_4)_3$

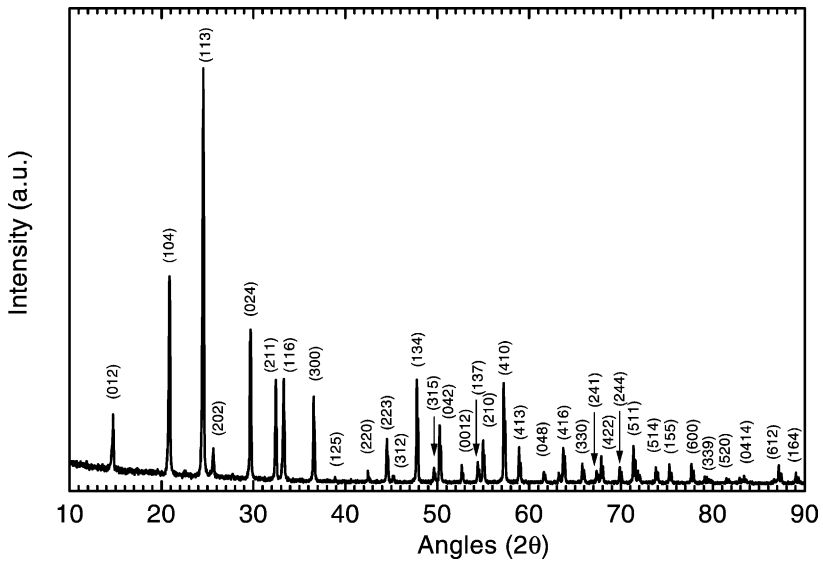

Fig. 1. X-ray diffraction pattern of $LiTi_2(PO_4)_3$ NASICON powders.

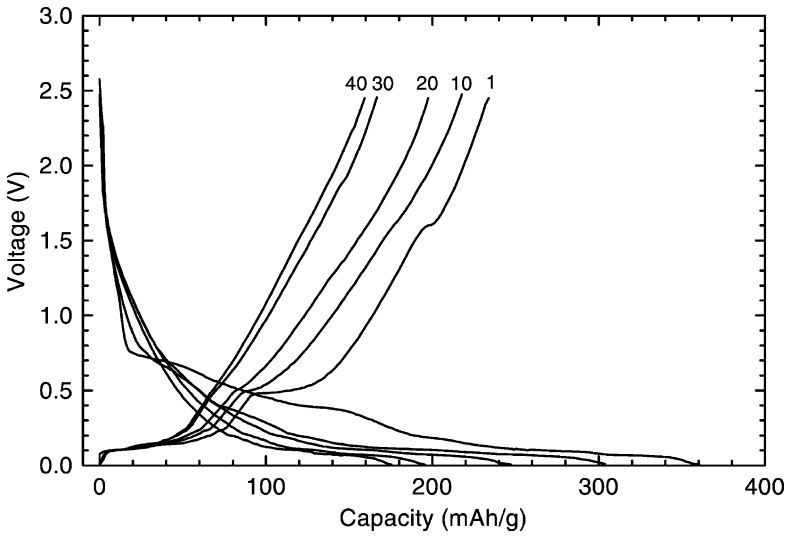

Fig. 2. Charge–discharge profiles of Li|LiPF$_6$ (EC + DMC)|LiTi$_2$(PO$_4$)$_3$ cell in voltage range 0–2.5 V. Current density: 0.1 mA cm^{-2}.

in the first lithiation process. Therefore, it is proposed that [PO$_4$] tetrahedra possibly also take part in the redox reaction to accept and donate electrons when lithium ions intercalate and de-intercalate in the LiTi$_2$(PO$_4$)$_3$ structure. At this stage, here is no direct physical evidence to confirm this proposal, but some support for the proposal is provided from studies by Ceder and coworkers [15,16] which indicate that oxygen atoms, rather than transition-metal ions, function as electron acceptors upon insertion of Li into metal-oxides and metal-dichalcogenides. Also, data from Li nuclear magnetic resonance (NMR) measurements also demonstrated that there is significant oxygen participation during the insertion of Li in TCO glass [17]. The situation for Li insertion in LiTi$_2$(PO$_4$)$_3$ NASICON is similar.

A quasi-open-circuit potential (OCV) versus composition curve was obtained by the galvanostatic intermittent titration technique (GITT). The Li|LiTi$_2$(PO$_4$)$_3$ cell was discharged to a desired value of x in Li$_{1+x}$Ti$_2$(PO$_4$)$_3$ at a constant current density of 20 μA cm^{-2} and then relaxed for 2 h. The final voltage of the cell was recorded as the OCV for that composition. The variation of OCVs versus inserted lithium composition x in the Li$_{1+x}$Ti$_2$(PO$_4$)$_3$ electrode is shown in Fig. 3. The maximum inserted Li is still about 5.2 mol per mole of Li$_{1+x}$Ti$_2$(PO$_4$)$_3$ even under quasi-equilibrium discharging condition.

The rate of capacity decay is related to the voltage range of cycling. Therefore, the cycling performance can be improved by limiting the voltage range of charge and discharge. Li|LiTi$_2$(PO$_4$)$_3$ cells were cycled in a voltage range 0.25–1.2 V. Surprisingly, the cells displayed excellent capacity retention (as shown in Fig. 4). During the first cycle, approximately by 80% of the initial inserted lithium is reversibly extracted during the first charge. After the first cycle, the reversibility of the electrode was much better than that cycled between 0 and 2.5 V.

The kinetic process of lithium insertion into LiTi$_2$(PO$_4$)$_3$ NASICON can be determined by ac impedance measurements. These were performed on the LiTi$_2$(PO$_4$)$_3$ electrode at different SoDs. The impedance spectra are presented in Fig. 5, from which the R_{CT} and exchange current density ($i_0 = RT/nFR_{CT}$) can be deduced. One semicircle is observed for the LiTi$_2$(PO$_4$)$_3$ electrode in the OCV state (no Li insertion). After Li intercalation, two semicircle are observed. The first semicircle is generally considered to contribute to the charge-transfer process and double-layer capacitance. The second semicircle is caused by a surface layer formed on the electrode, which is found on the carbonaceous electrode. The surface layer is formed when discharging the electrode below a potential of ~0.8 V versus Li/Li$^+$ due to the decomposition of the organic electrolyte. This has been confirmed by FTIR [18]. When Li insertion reaches $x > 2$ ($E \leq 0.2$ V versus Li/Li$^+$), however, the second semicircle disappears as shown in Fig. 5(c). This may be due to damage of the surface layer at low potential. The ac impedance spectra for SoDs of $x = 2.6$ and $x = 5.2$

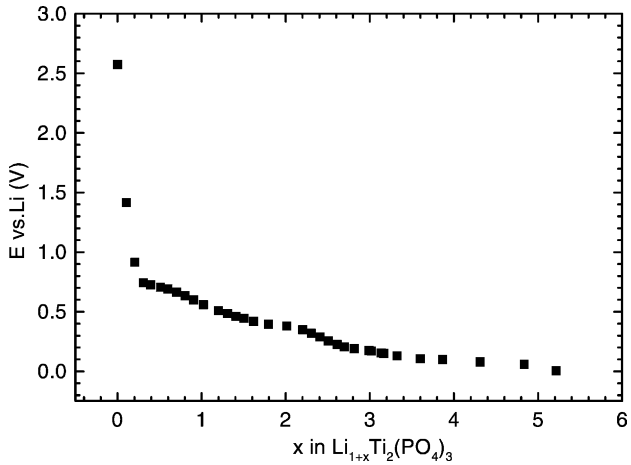

Fig. 3. Open-circuit potential vs. inserted lithium composition x in LiTi$_2$(PO$_4$)$_3$, obtained via GITT technique.

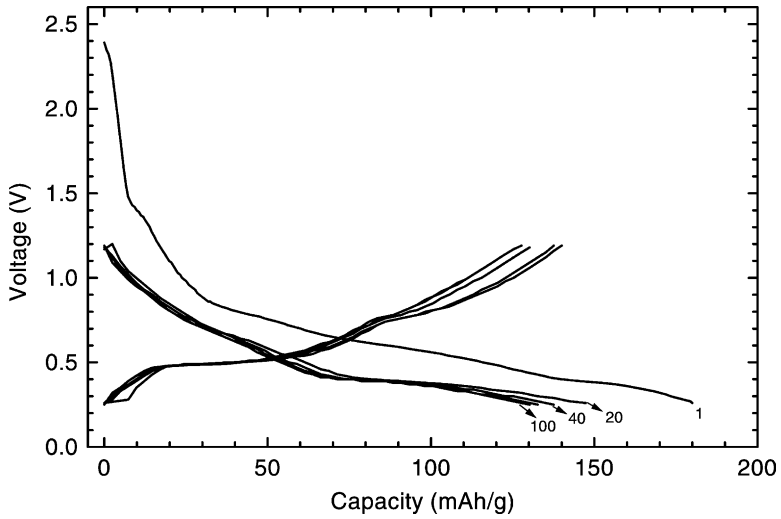

Fig. 4. Cycle profiles of Li|$LiPF_6$ (EC + DMC)|$LiTi_2(PO_4)_3$ cell with voltage cut-off between 0.25 and 1.2 V.

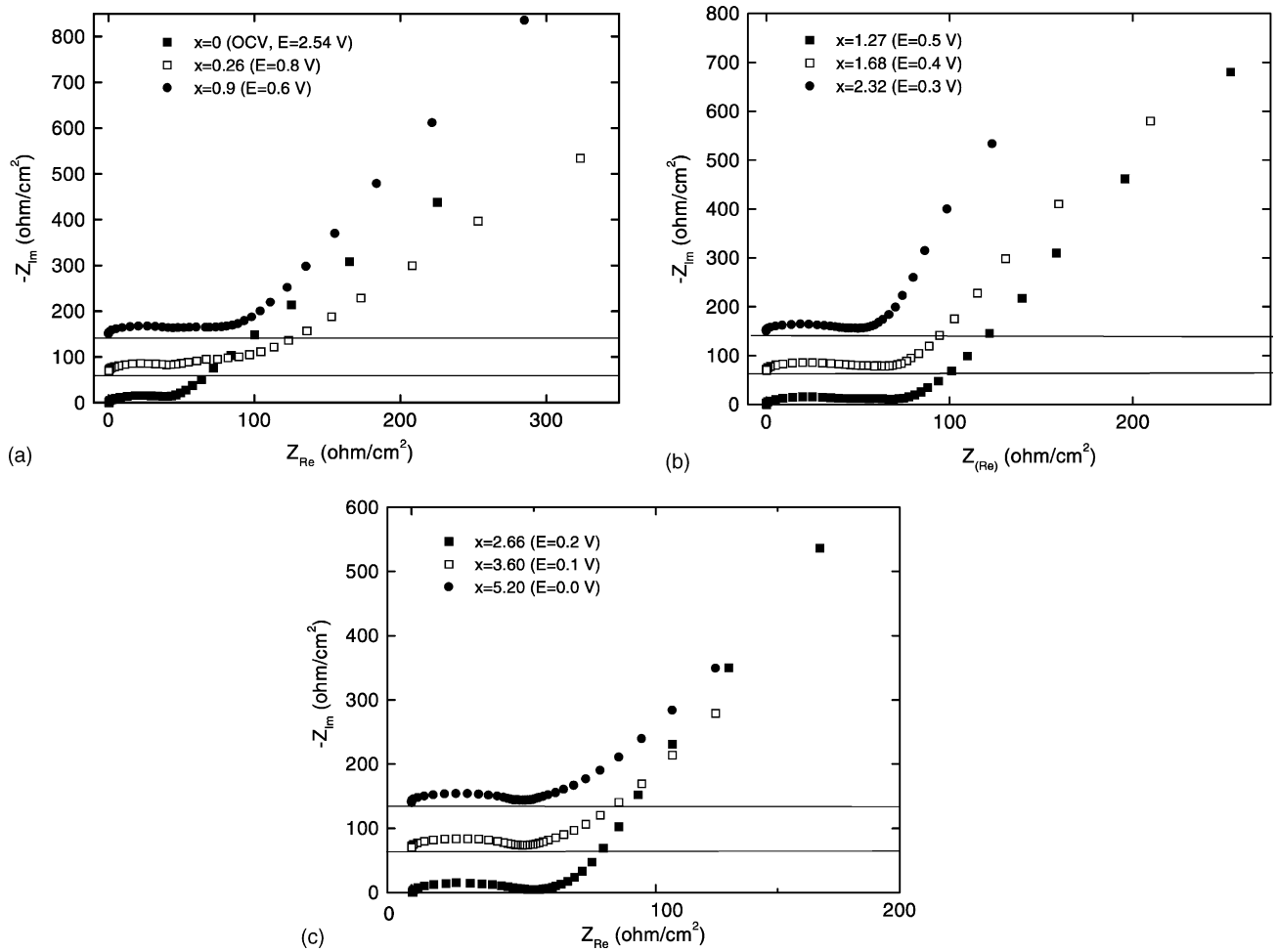

Fig. 5. (a–c) The ac impedance spectra for $LiTi_2(PO_4)_3$ electrode in different SoDs. SoD is expressed as the amount of inserted Li in $Li_{1+x}Ti_2(PO_4)_3$. Potentials (*E*) refer to potential of $Li_{1+x}Ti_2(PO_4)_3$ electrode vs. Li reference electrode.

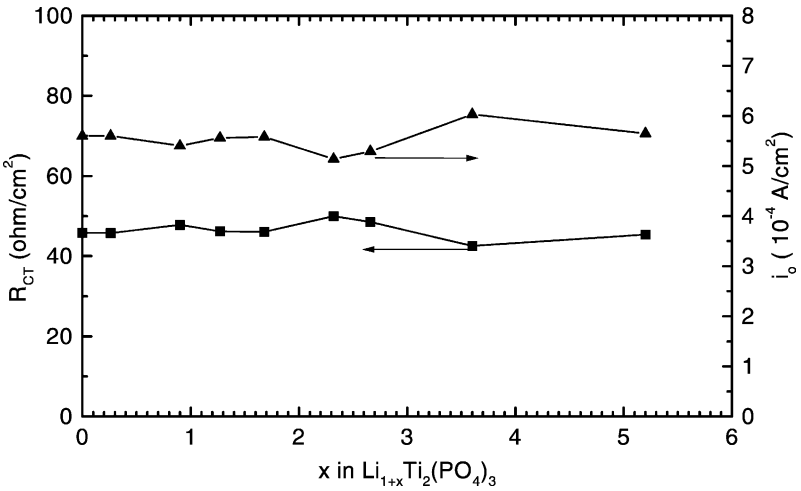

Fig. 6. Charge-transfer resistance (R_{CT}) and exchange current density (i_0) as function of SoD for $LiTi_2(PO_4)_3$ electrode.

are almost same. The R_{CT} and exchange current i_0 at different SoDs are estimated from the spectra and are shown in Fig. 6. The values of R_{CT} and the exchange current density i_0 are almost invariant, regardless the SoD. It is suggested that the reaction for lithium insertion in $LiTi_2(PO_4)_3$ proceeds as

$$x\mathrm{Li}^+ + x\mathrm{e}^- + \mathrm{LiTi_2(PO_4)_3} \rightarrow \mathrm{Li}_{1+x} + \mathrm{Ti_2(PO_4)_3} \quad (2)$$

The exchange current i_0 for the above reaction can be expressed by [19]

$$i_0 = nFk_sC_1^{(1-\alpha)}C_2^{\alpha} \quad (3)$$

where k_s is the reaction constants, C_1 and C_2 are the activities of Li^+ in the electrolyte and NASICON solid solution, respectively. C_1 can be taken to be constant during the insertion reaction. Since ac impedance studies showed i_0 to be invariant with Li insertion, C_2 should remain constant according to Eq. (3). It is considered that the inserted Li^+ ions occupy the interstitials or conducting channels, and this does not have an influence on the physical environment of Li^+ in $LiTi_2(PO_4)_3$. The unique structure characteristics of the NASICON skeleton with large numbers of interstitials and channels could be a contributing factor.

The kinetics for reaction (2) above are limited by Li diffusion in the host materials. The lithium diffusion coefficient, D_{Li}, in the $LiTi_2(PO_4)_3$ electrode can be calculated from the following formula which is based on a semi-infinite boundary condition:

$$D_{\mathrm{Li}} = \frac{1}{2}\left[\frac{V_m}{FS\sigma}\frac{dE}{dx}\right]^2 \quad (4)$$

where V_m is the molar volume of $LiTi_2(PO_4)_3$ (131 cm^3 mol^{-1}), dE/dx is the slope of the GITT curve at each x value, S is the apparent geometric area, σ is the Warburg coefficient.

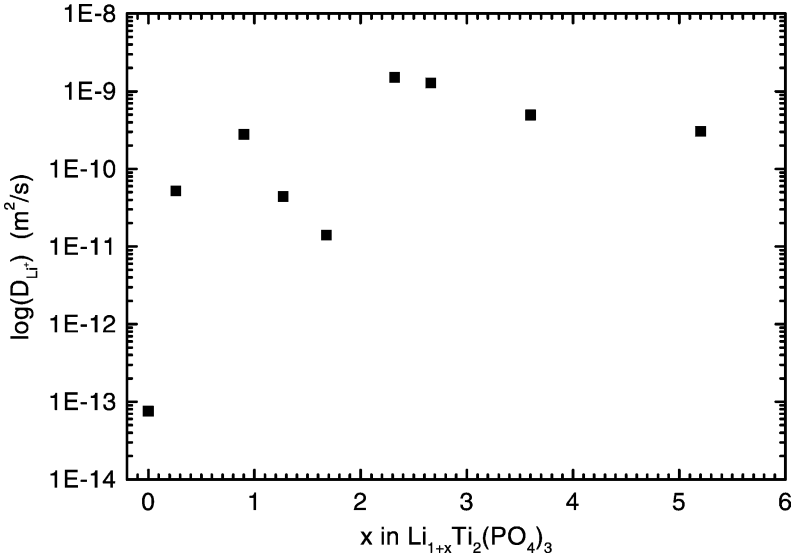

Fig. 7. Variation of Li^+ diffusion coefficient (D_{Li}) with SoD in $LiTi_2(PO_4)_3$ NASICON skeleton.

Values of D_{Li} at different SoDs are presented in Fig. 7. The D_{Li} at the OCV undischarged state is $7.6 \times 10^{-14}\,m^2\,s^{-1}$. After discharging, D_{Li^+} is in the range 1.4×10^{-11} to $1.2 \times 10^{-9}\,m^2\,s^{-1}$ which are much higher values than those for other intercalation materials such as $LiCo_yMn_{2-y}O_4$ for which D_{Li} is between 9.20×10^{-14} and $2.6 \times 10^{-12}\,cm^2\,s^{-1}$ and λ-MnO_2, where D_{Li} is between 1.9×10^{-12} and $3.1 \times 10^{-11}\,cm^2\,s^{-1}$ [20,21]. The conducting channels and interstitials in the NASICON structure could facilitate Li diffusion and, thereby, induce a high lithium diffusion coefficient.

4. Conclusions

The lithium insertion properties of $LiTi_2(PO_4)_3$ NASICON have been investigated. A maximum of about 5.2 mol Li-ions can be electrochemically intercalated per mole of $LiTi_2(PO_4)_3$ structure. Electrochemical impedance spectroscopy demonstrates that the Li diffusion coefficients in $LiTi_2(PO_4)_3$ are very high. This is considered to be related to the NASICON structure with interstitials and conducting channels. The exploration of NASICON materials could provide new electrode materials for lithium-ion batteries.

Acknowledgements

Financial support from Department, Education, Training and Youth Affairs, Australia is gratefully acknowledged.

References

[1] H. Kohler, H. Schulz, O. Melnikov, Mater. Res. Bull. 18 (1983) 1143–1152.
[2] B.V.R. Chowdari, K. Radhakrishna, K.A. Thomas, G.V. Subba Rao, Mater. Res. Bull. 24 (1989) 221–229.
[3] A. Leclaire, M.M. Borel, A. Grandin, B. Raveau, Mater. Res. Bull. 26 (1991) 207–221.
[4] Y. Miyajima, Y. Saito, M. Matsuoka, Y. Yamamoto, Solid State Ionics 84 (1996) 61–64.
[5] H.E. Sugimoto, N. Imanaka, G.-Y. Adachi, J. Electrochem. Soc. 137 (1990) 1023.
[6] C. Verissimo, F.M.S. Garrido, O.L. Alves, P. Calle, A. Martinez-Juarez, J.E. Iglesias, J.M. Rojo, Solid State Ionics 100 (1997) 127–134.
[7] E.R. Losilla, S. Bruque, M.A.G. Aranda, L. Moreno-Real, E. Morin, M. Quarton, Solid State Ionics 112 (1998) 53–62.
[8] K. Kasthuri Rangan, J. Gopalakrishnan, J. Solid State Chem. 109 (1994) 116–121.
[9] C.C. Torardi, E. Prince, Mater. Res. Bull. 21 (1986) 719.
[10] A. Manthiram, J.B. Goodenough, J. Solid State Chem. 71 (1987) 349–360.
[11] A.K. Padhi, C. Masquelier, K.S. Nanjundaswamy, J.B. Goodenough, Meeting Abstracts, 1997 Joint International Meeting, The Electrochemical Society, Paris, France, 31 August–5 September 1997, p. 88.
[12] Joint Commission on Powder Diffraction Standards (JCPDS) Card No. 35-754, International Center for Diffraction Data, Newtown Square, PA, USA.
[13] T. Ohzuku, A. Ueda, N. Yamamoto, J. Electrochem. Soc. 142 (1995) 1431–1435.
[14] D. Peramunage, K.M. Abraham, J. Electrochem. Soc. 145 (1998) 2609.
[15] M.K. Aydinol, A.F. Kohan, G. Ceder, K. Cho, J. Joannopoulos, Phys. Rev. B56 (1997) 1354–1365.
[16] G. Ceder, Y.-M. Chiang, D.R. Sadoway, M.K. Aydinol, Y.-I. Jiang, B. Huang, Nature 392 (1998) 694.
[17] G.R. Goward, F. Leroux, W.P. Power, G. Ourrard, W. Dmowski, T. Egami, L.F. Nazar, Electrochem. Solid State Lett. 2 (1999) 367–370.
[18] Y. Matsumura, S. Wang, J. Mondori, J. Electrochem. Soc. 142 (1995) 2914.
[19] Z. Galus, Fundamentals of Electrochemical Analysis, Wiley, New York, 1976, p. 67.
[20] H. Kanoh, Q. Feng, T. Hirotsu, K. Ooi, J. Electrochem. Soc. 143 (1996) 2610.
[21] P. Arora, B.N. Popov, R.E. White, J. Electrochem. Soc. 145 (1998) 807.